This is the accepted manuscript made available via CHORUS. The article has been published as:

Observation of gapless Dirac surface states in ZrGeTe

M. Mofazzel Hosen, Klauss Dimitri, Alex Aperis, Pablo Maldonado, Ilya Belopolski, Gyanendra Dhakal, Firoza Kabir, Christopher Sims, M. Zahid Hasan, Dariusz Kaczorowski, Tomasz Durakiewicz, Peter M. Oppeneer, and Madhab Neupane

Phys. Rev. B **97**, 121103 — Published 7 March 2018

DOI: 10.1103/PhysRevB.97.121103

Observation of Gapless Dirac Surface States in ZrGeTe

M. Mofazzel Hosen,[1] Klauss Dimitri,[1] Alex Aperis,[2] Pablo Maldonado,[2] Ilya Belopolski,[3] Gyanendra Dhakal,[1] Firoza Kabir,[1] Christopher Sims,[1] M. Zahid Hasan,[3] Dariusz Kaczorowski,[4] Tomasz Durakiewicz,[5,6] Peter M. Oppeneer,[2] and Madhab Neupane*[1]

[1]*Department of Physics, University of Central Florida, Orlando, Florida 32816, USA*
[2]*Department of Physics and Astronomy, Uppsala University, P. O. Box 516, S-75120 Uppsala, Sweden*
[3]*Joseph Henry Laboratory and Department of Physics, Princeton University, Princeton, New Jersey 08544, USA*
[4]*Institute of Low Temperature and Structure Research, Polish Academy of Sciences, 50-950 Wroclaw, Poland*
[5]*Condensed Matter and Magnet Science Group, Los Alamos National Laboratory, Los Alamos, NM 87545, USA*
[6]*Institute of Physics, Maria Curie - Sklodowska University, 20-031 Lublin, Poland*

(Dated: February 23, 2018)

The experimental discovery of the topological Dirac semimetal establishes a platform to search for various exotic quantum phases in real materials. ZrSiS-type materials have recently emerged as topological nodal-line semimetals where gapped Dirac-like surface states are observed. Here, we present a systematic angle-resolved photoemission spectroscopy (ARPES) study of ZrGeTe, a non-symmorphic symmetry protected Dirac semimetal. We observe two Dirac-like gapless surface states at the same $\bar{X}$ point of the Brillouin zone. Our theoretical analysis and first-principles calculations reveal that these are protected by crystalline symmetry. Hence, ZrGeTe appears as a rare example of a naturally fine tuned system where the interplay between symmorphic and non-symmorphic symmetry leads to rich phenomenology, and thus opens for opportunities to investigate the physics of Dirac semimetallic and topological insulating phases realized in a single material.

The experimental discovery of the topological insulator (TI) [1–5] tremendously motivated research in topological Dirac semimetals (TDS) which offer a platform for realizing many exotic physical phenomena such as high electron mobility and magnetoresistance. The TDSs [6–17] are characterized by symmetry protected band touchings at certain k-points of the Brillouin zone (BZ) or 1D lines or loops (topological nodal-line semimetals) [18–33]. Importantly, this point or line contact can be lifted by tuning the spin-orbit coupling (SOC) strength [32–34].

A distinct class of TDS is characterized by the presence of non-symmorphic symmetries [11, 12, 24]. Such non-symmorphic materials possess forced band degeneracies at high symmetry points of the BZ as a consequence of fractional translational symmetry combined with a point group symmetry such as mirror or rotational symmetry. In the presence of time reversal symmetry, the Dirac points are pinned at the time reversal invariant momenta of the BZ [12]. This forced band degeneracy cannot be lifted by any perturbation including spin-orbit coupling. Such robust bulk Dirac points have been observed in 3D systems [24, 25] while a non-symmorphic symmetry protected nodal line phase has been reported in ZrSiS-type materials [35, 36] together with the presence of a gapped Dirac cone surface state.

Being essential for TDS, the space group symmetry protection plays a pivotal role in topological insulators (TIs), as well. While the so-called non-symmorphic TIs [37–39] are currently sought after, their symmorphic counterparts, i.e. the topological crystalline insulators (TCIs), are already well established [40–42] after they were first theoretically predicted [43]. A striking feature of TCIs is that they can host band inversions at multiple non-equivalent time-reversal invariant momenta (TRIMs) of their bulk BZ that, depending on the orientation of the cleaved surface, may project onto the same TRIM of the surface BZ [44]. If the number of such projected points is even, then one would naively expect a trivial insulating phase since the overall Z_2 [45] indices would vanish. However, if the cleaved surface preserves a crystalline symmetry of the bulk such as a rotation or mirror, then this extra symmetry can protect the surface states, thus giving rise to the TCI phase. Interestingly, such gapless surface states may exhibit multifold, anisotropic Weyl-like dispersions that are more complex than the usual strong or weak TI surface states [44].

So far, little is known about the interplay of TDS and TI phases and whether these two phases can coexist in the same non-symmorphic material. In this letter, we report a systematic investigation of ZrGeTe, a member of the ZrSiS-type material family, combining both ARPES measurements and first-principles calculations, and establish ZrGeTe as a new material with multiple gapless Dirac fermionic surface states, reminiscent of that encountered in TCIs. We show that in contrast to typical TCIs, in ZrGeTe the gapless surface states stem from a double band inversion that takes place at a single non-equivalent bulk TRIM, due to an inversion between two non-symmorphic symmetry protected bulk Dirac points. At the surface, the residual symmorphic part of this symmetry remains and protects the resulting surface states. Our findings suggest that ZrGeTe can aptly function as a new platform for studying exotic properties caused by coexistence of TDS and TI phases in one material, due to the interplay between symmorphic and non-symmorphic symmetry.

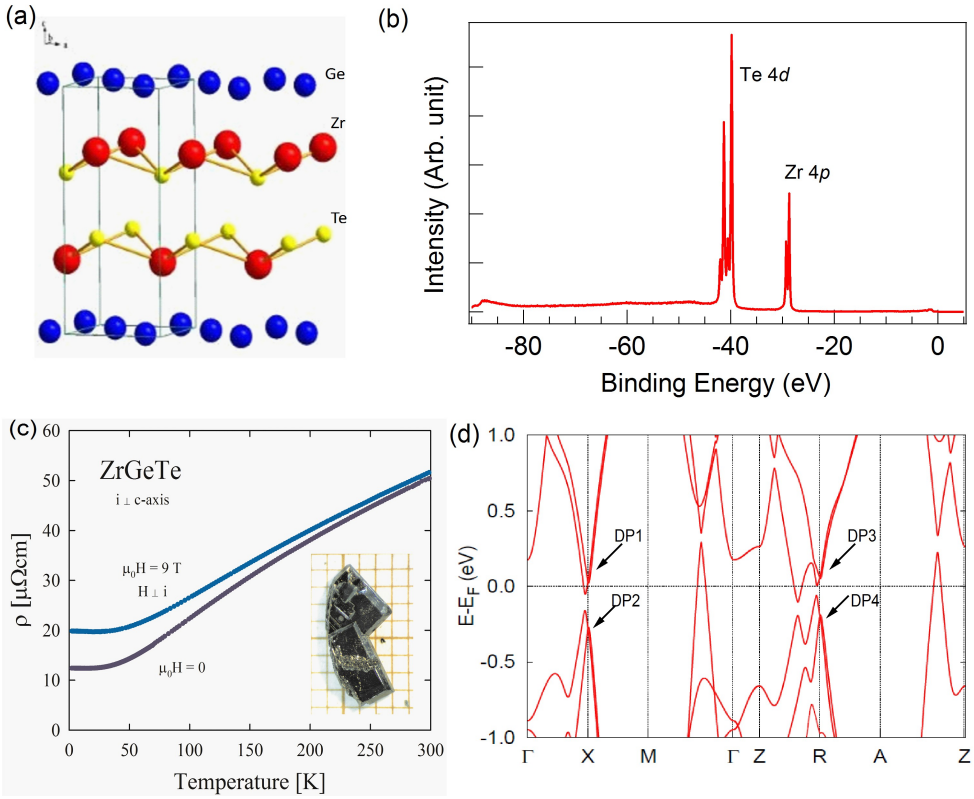

FIG. 1: Crystal structure and sample characterization of ZrGeTe. (a) Tetragonal crystal structure of ZrGeTe. The Zr layers are separated by two neighboring Te layers, which are both sandwiched between the Ge atoms forming a square net. (b) Spectroscopically measured core-level of ZrGeTe. Sharp peaks of Te 4*d* and Zr 4*p* are observed. (c) Temperature variation of the electrical resistivity of ZrGeTe within the tetragonal plane measured in zero magnetic field and in a field of 9 T applied along the c-axis. Inset shows a single crystal of ZrGeTe. (d) *Ab initio* calculated band structures of ZrGeTe along high symmetry directions. Bulk Dirac points (DP) are indicated in the plot.

Single crystals of ZrGeTe were grown by chemical vapor transport method using iodine as transporting agent [46]. Similar to the MSiX, where M = Zr, Hf and X = S, Se, Te, respectively, it also crystallizes in the PbFCl-type crystal structure with space group $P4/nmn$ (No. 129). Fig. 1(a) illustrates the layered [52] crystal structure of ZrGeTe. The Zr atom layers are separated by two Te layers and the Zr-Te terminals are sandwiched between a Ge square net. The bond between Zr-Te is relatively weak compared to the bond between Zr-Ge hence providing a natural cleaving plane between the two neighboring Zr-Te layers and therefore cleaves easily along the (001) plane. Furthermore, the square Si-net provides a natural glide plane and the crystal preserves two sets of non-symmorphic symmetry. Fig. 1(b) presents the spectroscopic core level measurement of ZrGeTe. We observe the sharp peaks of Zr 4*p* (∼28.5 eV) and Te 4*d* (∼40 eV) of ZrGeTe, which further indicate the excellent quality of the samples used for our measurements. As shown in Fig. 1(c), ZrGeTe exhibits metallic-like electrical conductivity, with the temperature dependence similar to that reported for ZrSiTe [33]. At room temperature, the resistivity measured within the basal plane of the tetragonal unit cell (i ⊥ c-axis) amounts to 50 $\mu\Omega$cm. With decreasing temperature, it decreases smoothly down to about 12 $\mu\Omega$cm at 2 K. In magnetic field of 9 T, applied along the c-axis, the overall character of ρ(T) hardly changes, in striking contrast to the behavior in ZrSiS and ZrSiSe [17, 33], yet fairly reminiscent to the case of ZrSiTe [33]. At 2 K, the transverse (H ⊥ i) magnetoresistance of ZrGeTe, defined as MR = [ρ(T, μ_0H = 9 T) - ρ(T,0]/ρ(T,0), is positive and attains about 60%. It is twice larger than the MR in ZrSiTe [33], yet a few orders of magnitude smaller than in the other Si-bearing counterparts [17, 33]. Fig. 1(d) presents the calculated bulk bands along various high symmetry directions.

To unveil the detailed electronic structure of ZrGeTe, we present our ARPES measured electronic structure in Figs. 2 and 3. Fig. 2a shows the Fermi surface map and constant energy contours measured at the ALS beamline 10.0.1 at a photon energy of 60 eV and temperature of 15 K. Experimentally we observe a diamond shaped Fermi surface around the Γ point and circular shaped Fermi pockets at the X point of the BZ. Moving toward higher binding energies the diamond shaped Fermi surface becomes disconnected resembling an inner diamond within an outer diamond. The two diamond shaped Fermi surfaces are clearly disconnected along the M-Γ-M direction. At around 450 meV the circular shaped Fermi pockets shrink into a point-like state located around the binding energy of the Dirac points. This reveals the electron like nature of the bands around the X points of the BZ. Fig. 2b displays the theoretically calculated counterpart of fig. 2a showing excellent agreement with the experiment. Moreover, our first-principles calculations identify the surface origin of the bands around the X points (see below) which is also consistent with previously reported data on other materials of this family [5, 24, 35, 36].

To reveal the nature of the states around the X point

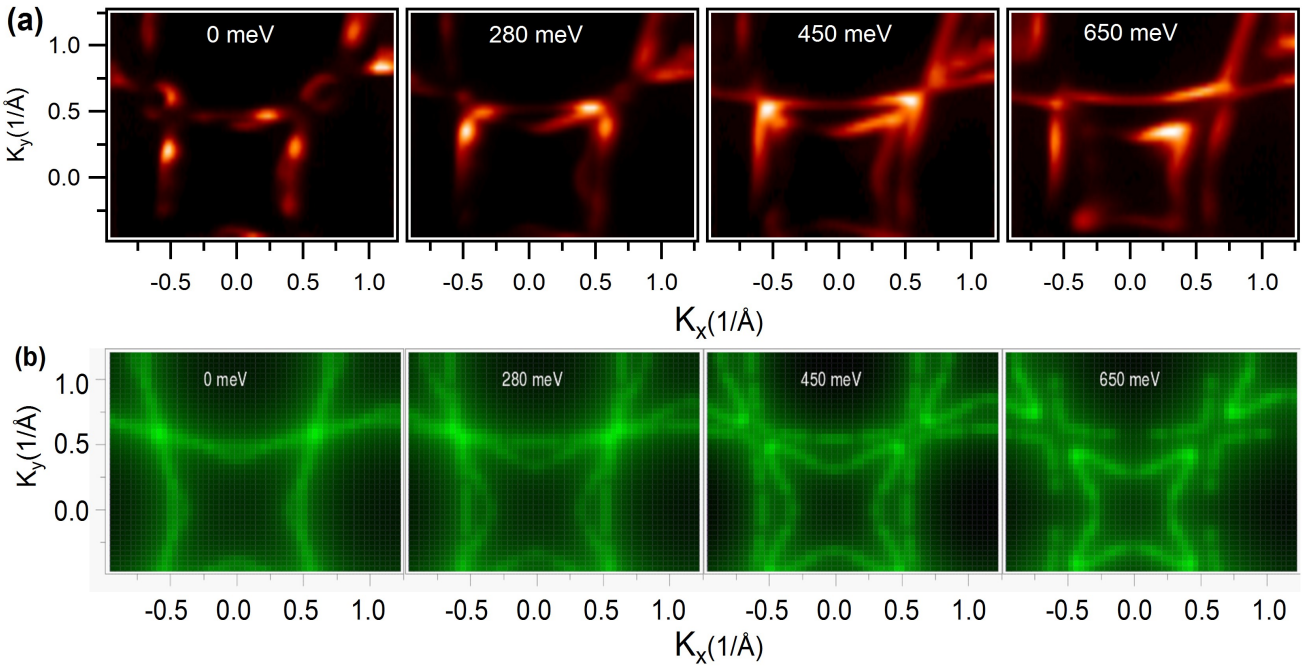

FIG. 2: Fermi surface map and constant energy contours of ZrGeTe. (a) Measured Fermi surface and constant energy contours. The binding energy values are noted in the plots. All measurements were performed at the ALS beamline 10.0.1 at a temperature of ∼15 K. (b) *Ab initio* calculated Fermi surface map and constant energy contours. The binding energy values are noted in the plots.

and along various high-symmetry directions, it is necessary to perform photon energy dependent ARPES measurements as shown in Fig. 3. Fig. 3(a) shows the Fermi surface map and the high-symmetry points are noted in the plot. Fig. 3(b) shows the photon energy dependent dispersion maps along the M-Γ-M direction. It shows good qualitative agreement with our calculated dispersion map as shown in Fig. 3(c). Our calculations predicted a nodal-line state along the M-Γ-M direction, however, it is located above the Fermi level. Fig. 3(d) shows the dispersion maps along the Γ-X-Γ direction at various photon energies (see also supplementary informations [46]). By comparing with the slab calculations along this direction [see Fig. 3(e)], we can clearly identify the surface [blue color in Fig. 3(e,g)] and bulk [red color in Fig. 3(e,g)] originated states. The upper V shape in the experimental data clearly originates from the surface state, however in the $\mathcal{M}$ shaped states, the bulk states interfere with the surface states. An important point to notice here is that our calculations predicted a gapless Dirac surface state at the X point over a wide energy range along the M-X-M direction, which is consistent with our experimental observations. To further confirm this, we have performed photon energy dependent dispersion mapping along this direction. Fig. 3(f) represents the dispersion maps along the M-X-M high symmetry direction at different photon energies, as noted on the plots. The Dirac points are observed to be located at around 400 meV. A hole-like band is seen around at 1.3 eV binding energy changing the shape with the change of photon energy which infers the bulk band. We note the presence of bright intensity in the vicinity of the Dirac point in Fig. 3(f). As we discuss further below, this feature is due to the interference between the near degenerate Weyl states that form the gapless surface states [46]. The experimentally observed states are reproduced nicely in our calculations. The surface states do not show any gap as compared to the bulk states [see Fig. 3(f)] which is also consistent with our band calculations [see Fig. 3(e,g)]. The presence of eight surface states in total in Fig. 3(g) is due to the fact that in the slab calculations there is a top and a bottom surface contributing.

Our calculation reveals that ZrGeTe is a Dirac semimetal with bulk Dirac crossings at X and R, in accordance with other members of this family [35]. This picture is consistent with our bulk calculations where these crossings are found to occur near the Fermi level at energies around 83 meV and -200 meV, respectively (DP1–4 in Fig. 1(d)). These fourfold bulk DPs are protected by non-symmorphic symmetry ($\widetilde{M}_{\hat{z}} : \{m_{001}|1/2\ 1/2\ 0\}$) combined by time-reversal and inversion ($P\Theta$) symmetry [12]. Usually, TDS surface states are expected to manifest as higher dimensional objects, like e.g. Fermi arcs [31]. In stark contrast, the surface states reported here are Dirac-like and emerge at the $\bar{X}$ point of the surface BZ at an energy position that is located between the bulk

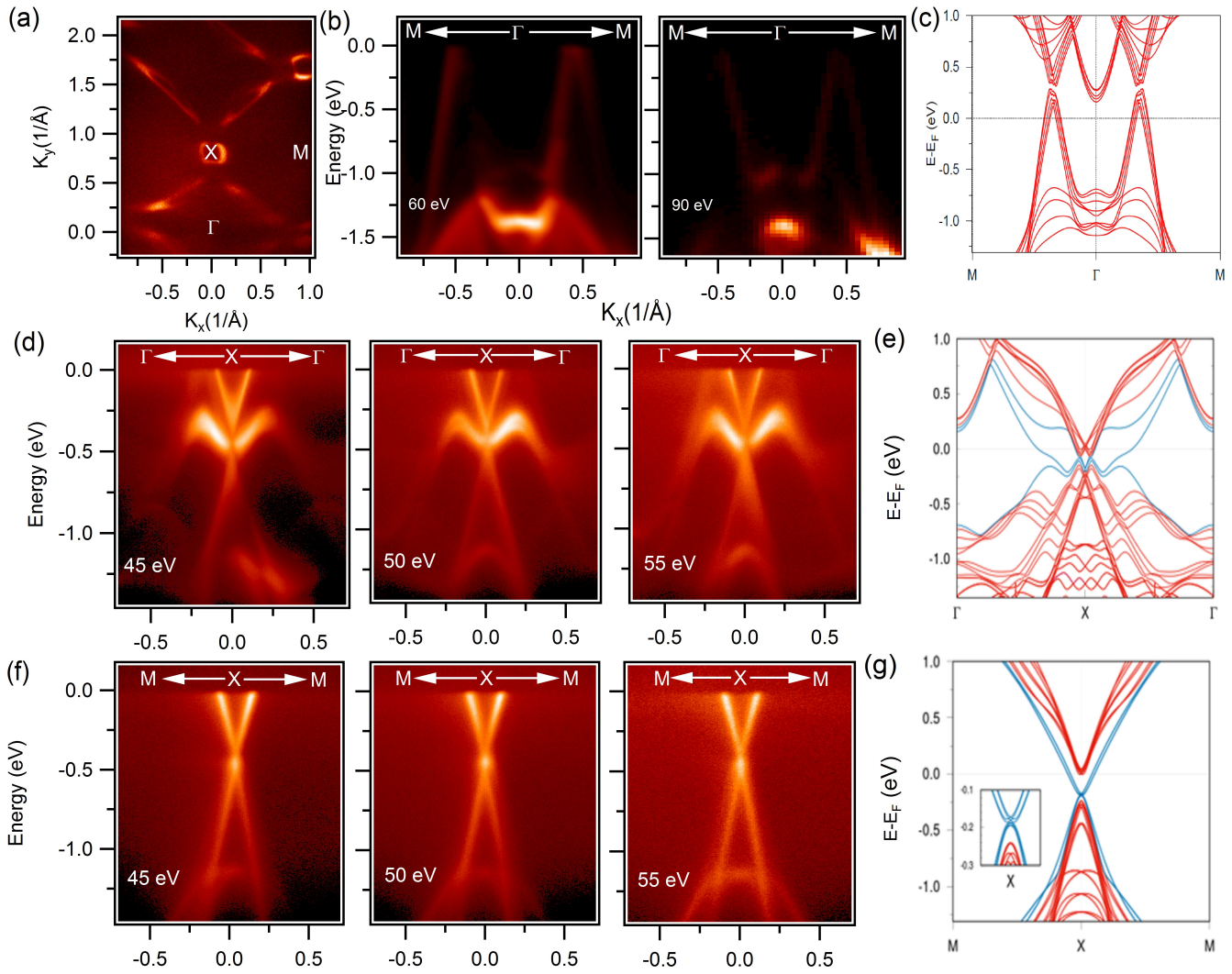

FIG. 3: Observation of gapless Dirac fermion state. (a) Measured Fermi surface at a photon energy of 40 eV. High-symmetry points are indicated in the plot. (b) Measured dispersion maps along the M-Γ-M direction at photon energies of 60 eV and 90 eV, respectively. (c) *Ab initio* calculations showing the dispersion map along the M-Γ-M high-symmetry direction. (d) Photon energy dependent ARPES dispersion maps along the Γ-X-Γ direction. The photon energies are noted on the plots. **(e)** Calculated dispersion map along the high-symmetry direction Γ-X-Γ. (f) ARPES energy-momentum dispersion maps measured with various photon energies along the M-X-M direction. Linearly dispersive states are observed that do not show dispersion with a dependence on photon energy. The photon energies are noted on the plots. (g) Calculations showing the dispersion map along the M-X-M high-symmetry direction. The inset show a zoomed in plot of bands around the X point which clearly shows the band touching, in qualitative agreement with the experimental data. All experiments were performed at the ALS end-stations 10.0.1 and 4.0.3 at a temperature of $\sim 15-20\,$K.

Dirac crossings. These characteristics are reminiscent to the surface states of topological insulators.

In ZrGeTe there exists a momentum dependent gap between bands forming DP1, 2 and DP3, 4 [Fig. 1(d)] throughout the whole bulk BZ. Our calculations yield that the bands forming the DP3 and DP4 [see Fig. 1(d)] are inverted leading to a double band inversion at R. Each band inversion leads to the set of weak topological indices $(\nu_0;\nu_1\,\nu_2\,\nu_3)$=(0; 1 1 0) which would give rise to gapless Dirac surface states at the equivalent $\bar{X}$ points of the (001) surface. Since there are two band inversions in total, the overall parity does not change and this leads to vanishing overall Z_2 indices, unless an additional symmetry can protect the surface states thus leading to a TCI phase [43, 44].

Our analysis gives that each band inversion is characterized by a different eigenvalue of the non-symmorphic symmetry operator that protects each bulk DP. Observing that $\widetilde{M}_{\hat{z}} = PC_{2\hat{z}}$, with $C_{2\hat{z}} : \{2_{001}|1/2\ 1/2\ 0\}$, we

have that at the (001) surface where P is broken, $\widetilde{M_{\hat{z}}}$ is broken as well, but $C_{2\hat{z}}$ remains intact. The latter is a crystalline symmetry that protects the resulting gapless surface states, leading to similar phenomenology as in TCIs. In fact, taking into account all remaining symmetries of the (001) surface, the resulting $k \cdot p$ model near $\bar{X}$ is similar to the archetypical one for TCIs [44], leading to a pair of anisotropic Weyl-like surface states at $\bar{X}$. The surface states given by our *ab initio* slab calculations disperse linearly (quadratically) along the $\bar{\Gamma} - \bar{X}$ ($\bar{M} - \bar{X}$) direction thus complying with this picture. Moreover, we find that the expected surface mass term [44] in the case of ZrGeTe is small so that the two surface states are near degenerate, thus giving rise to the bright spot seen in our ARPES data at the crossing point as shown in Fig. 3(f).

Hence, our analysis proposes that ZrGeTe is the first topological material where TDS and TCI phases coexist under the protection of space-group symmetry. Notably, and in contrast to the usual TCIs, ZrGeTe is the first paradigm of a TCI that stems from multiple band inversions at the same time-reversal invariant momentum of the bulk BZ. A plausible reason why gapless surface states occur in ZrGeTe but not in other MSiX materials, are the different atomic size of Ge in contrast to Si and/or enhanced spin-orbit coupling that may allow for band inversions to occur. In this respect, ZrGeTe appears as a rare example of a naturally fine-tuned system so that it can exhibit such rich phenomenology.

In conclusion, we performed systematic investigations of the ZrGeTe system. Our experimental ARPES data and *ab initio* calculations reveal the existence of twofold symmetry protected Dirac-like gapless surface states. Moreover, our calculations reveal the presence of a nodal-line state along the M-Γ-M direction. Our study thus highlights the existence of topological Dirac semimetal and topological insulator states in a single material, and opens up new prospects for studying the as yet unexplored interplay of these exotic quantum states.

M.N. is supported by the Air Force Office of Scientific Research under Award Number FA9550-17-1-0415 and the startup fund from UCF. T.D. is supported by NSF IR/D program. A.A., P.M., and P.M.O. acknowledge support from the Swedish Research Council (VR), the Röntgen-Ångström Cluster, and the Swedish National Infrastructure for Computing (SNIC). I.B. acknowledges the support of the NSF GRFP. Work at Princeton University is supported by the Emergent Phenomena in Quantum Systems Initiative of the Gordon and Betty Moore Foundation under Grant No. GBMF4547 (M.Z.H.) and by the National Science Foundation, Division of Materials Research, under Grants No. NSF-DMR-1507585 and No. NSF-DMR-1006492. We thank Sung-Kwan Mo and Jonathan Denlinger for beamline assistance at the LBNL.

[1] M. Z. Hasan and C. L. Kane, Rev. Mod. Phys. **82**, 3045 (2010).
[2] X.-L. Qi and S.-C. Zhang, Rev. Mod. Phys. **83**, 1057 (2011).
[3] M. Z. Hasan, S.-Y. Xu, and M. Neupane, (eds. Ortmann, F., Roche, S. & Valenzuela, S. O.) (John Wiley & Sons, New York, 2015).
[4] Y. Xia, D. Qian, D. Hsieh, L. Wray, A. Pal, H. Lin, A. Bansil, D. Grauer, Y. S. Hor, R. J. Cava, and M. Z. Hasan, Nat. Phys. **5**, 398 (2009).
[5] M. Neupane, A. Richardella, J. Sanchez-Barriga, S.Y. Xu, N. Alidoust, I. Belopolski, C. Liu, G. Bian, D. Zhang, D. Marchenko, A. Varykhalov, O. Rader, M. Leandersson, T. Balasubramanian, T.-R. Chang, H.-Tay Jeng, S. Basak, H. Lin, A. Bansil, N. Samarth, and M. Z. Hasan, Nat. Commun. **5**, 3841 (2014).
[6] Z. Wang, H. Weng, Q. Wu, Xi Dai, and Z. Fang, Phys. Rev. B **88**, 125427 (2013).
[7] M. Neupane, S.-Y. Xu, R. Sankar, N. Alidoust, G. Bian, C. Liu, I. Belopolski, T.-R. Chang, H.-T. Jeng, H. Lin, A. Bansil, F.-C. Chou, and M. Z. Hasan, Nat. Commun. **5**, 3786 (2014).
[8] Neupane, M. N. Alidoust, S.-Y. Xu, T. Kondo, Y. Ishida, D. J. Kim, C. Liu, I. Belopolski, Y. J. Jo, T-R. Chang, H-T. Jeng, T. Durakiewicz, L. Balicas, H. Lin, A. Bansil, S. Shin, Z. Fisk, and M. Z. Hasan, Nat. Commun. **4**, 2991 (2013).
[9] S. Borisenko, Q. Gibson, D. Evtushinsky, V. Zabolotnyy, B. Buchner, and R. J. Cava, Phys. Rev. Lett. **113**, 027603 (2014).
[10] B.-J. Yang and N. Nagaosa, Nat. Commun. **5**, 4898 (2014).
[11] S. M. Young, S. Zaheer, J. C. Y. Teo, C. L. Kane, E. J. Mele, and A. M. Rappe, Phys. Rev. Lett. **108**, 140405 (2012).
[12] S. M. Young and C. L. Kane, Phys. Rev. Lett. **115**, 126803 (2015).
[13] M. Z. Hasan, S.-Y. Xu, G. Bian, Phys. Scr. **T164**, 014001 (2015).
[14] Z. K. Liu, B. Zhou, Z. J. Wang, H. M. Weng, D. Prabhakaran, S. -K. Mo, Y. Zhang, Z. X. Shen, Z. Fang, X. Dai, Z. Hussain, and Y. L. Chen, Science **343**, 864 (2014).
[15] M. Neupane, N. Alidoust, M. M. Hosen, J.-X. Zhu, K. Dimitri, S.-Y. Xu, N. Dhakal, R. Sankar, I. Belopolski, D. S. Sanchez, T.-R. Chang, H.-T. Jeng, K. Miyamoto, T. Okuda, H. Lin, A. Bansil, D. Kaczorowski, F. C. Chou, M. Z. Hasan, and T. Durakiewicz, Nat. Commun. **7**, 13315 (2016).
[16] M. Neupane, M. M. Hosen, I. Belopolski, N. Wakeham, K. Dimitri, N. Dhakal, J.-X. Zhu, M. Z. Hasan, E. D Bauer, and F. Ronning, J. Phys.: Cond. Matter **28**, 23LT02 (2016).
[17] X. Wang, X. Pan, M. Gao, J. Yu, J. Jiang, J. Zhang,H. Zuo, M. Zhang, Z. Wei, W. Niu, Z. Xia, X. Wan, Y. Chen, F. Song, Y. Xu, B. Wang, G. Wang, and R. Zhang, Adv. Electron. Mater. **2**, 1600228 (2016).
[18] A. A. Burkov, M. D. Hook, and L. Balents, Phys. Rev. B **84**, 235126 (2011).
[19] M. Phillips and V. Aji, Phys. Rev. B **90**, 115111 (2014).
[20] H. Weng, Y. Liang, Q. Xu, R. Yu, Z. Fang, X. Dai, and

Y. Kawazoe, Phys. Rev. B **92**, 045108 (2015).
[21] Y. Kim, B. J. Wieder, C. L. Kane, and A. M. Rappe, Phys. Rev. Lett. **115**, 036806 (2015).
[22] L. S. Xie, L. M. Schoop, E. M. Seibel, Q. D. Gibson, W. Xie, and R. J. Cava., Appl. Phys. Lett. Mat. **3**, 083602 (2015).
[23] M. M. Hosen, K. Dimitri, A. K. Nandy, A. Aperis, R. Sankar, G. Dhakal, P. Maldonado, F. Kabir, C. Sims, F. C. Chou, D. Kaczorowski, T. Durakiewicz, P. M. Oppeneer, and M. Neupane, arXiv:1711.07390 (2017).
[24] L. M. Schoop, M. N. Ali, C. Straber, V. Duppel, S. S. P. Parkin, B. V. Lotsch, and C. R. Ast, Nat. Commun. **7**, 11696 (2016).
[25] M. Neupane, I. Belopolski, M. M. Hosen, D. S. Sanchez, R. Sankar, M. Szlawska, S.-Y. Xu, K. Dimitri, N. Dhakal, P. Maldonado, P. M. Oppeneer, D. Kaczorowski, F. C. Chou, M. Z. Hasan, and T. Durakiewicz, Phys. Rev. B **93**, 201104(R) (2016).
[26] R. Lou, J.-Z. Ma, Q.-N. Xu, B.-B. Fu, L.-Y. Kong, Y.-G. Shi, P. Richard, H.-M. Weng, Z. Fang, S.-S. Sun, Q. Wang, H.-C. Lei, T. Qian, H. Ding, S.-C. Wang, Phys. Rev. B **93**, 241104(R) (2016).
[27] Y.-Y Lv, B.-B. Zhang, X. Li, S.-H. Yao, Y. B. Chen, J. Zhou, S.-T. Zhang, M.-H. Lu, and Y.-F. Chen, arXiv:1604.01864 (2016).
[28] G. Bian, T.-R. Chang, R. Sankar, S.-Y. Xu, H. Zheng, T. Neupert, C.-K. Chiu, S.-M. Huang, G. Chang, I. Belopolski, D. S. Sanchez, M. Neupane, N. Alidoust, C. Liu, B. K. Wang, C.-C. Lee, H.-T. Jeng, C. Zhang, Z. Yuan, S. Jia, A. Bansil, F. C. Chou, H. Lin, and M. Z. Hasan, Nat. Commun. **7**, 10556 (2016).
[29] Y. Wu, L.-L.Wang, E. Mun, D. D. Johnson, D. Mou, L. Huang, Y. Lee, S. L. Budko, P. C. Canfield, and A. Kaminski, Nat. Phys **12**, 667?671 (2016).
[30] J. Hu, Z. Tang, J. Liu, X. Liu, Y. Zhu, D. Graf, Y. Shi, S. Che, C. N. Lau, J. Wei, and Z. Mao, Phys. Rev. Lett. **117**, 016602 (2016).
[31] D. Takane, Z. Wang, S. Souma, K. Nakayama, C. X. Trang, T. Sato, T. Takahashi, and Y. Ando, Phys. Rev. B **94**, 121108(R) (2016).
[32] J. Hu, Y. L. Zhu, D. Graf, Z. J. Tang, J. Y. Liu, and Z. Q. Mao, Phys. Rev. B **95**, 205134 (2017).
[33] M. M. Hosen, K. Dimitri, I. Belopolski, P. Maldonado, R. Sankar, N. Dhakal, G. Dhakal, T. Cole, P. M. Oppeneer, D. Kaczorowski, F. C. Chou, M. Z. Hasan, T. Durakiewicz, and M. Neupane, Phys. Rev. B **95**, 161101(R) (2017).
[34] R. Yu, Z. Fang, X. Dai, and H. Weng, Front. Phys. **12**, 127202 (2017).
[35] A. Topp, J. M. Lippmann, A. Varykhalov,V. Duppel, B. V. Lotsch, C. R. Ast, and L. M. Schoop, New J. Phys. **18**, 125014 (2016).
[36] C. Chen, X. Xu, J. Jiang, S. -C. Wu, Y. P. Qi, L. X. Yang, M. X. Wang, Y. Sun, N.B.M. Schrter, H. F. Yang, L. M. Schoop, Y. Y. Lv, J. Zhou, Y. B. Chen, S. H. Yao, M. H. Lu, Y. F. Chen, C. Felser, B. H. Yan, Z. K. Liu and Y. L. Chen, arXiv:1701.06888v1 (2016).
[37] C. Fang and L. Fu, Phys. Rev. B. **91**, 161105 (2015).
[38] K. Shiozaki, M. Sato, and K. Gomi, Phys. Rev. B. **91**, 155120 (2015).
[39] Z. Wang, A. Alexandradinata, R. J. Cava, and B. A. Bernevig, Nature **532**, 189-194 (2016).
[40] H. Hsieh, H. Lin, J. Liu, W. Duan, A. Bansil and L. Fu, Nat. Commun. **3**, 982 (2012).
[41] S.-Y. Xu, C. Liu, N. Alidoust, M. Neupane, D. Qian, I. Belopolski, J. D. Denlinger, Y. J. Wang, H. Lin, L. A. Wray, G. Landolt, B. Slomski, J. H. Dil, A. Marcinkova, E. Morosan, Q. Gibson, R. Sankar, F. C. Chou, R. J. Cava, A. Bansil and M. Z. Hasan, Nat. Commun. **3**, 1192 (2012).
[42] Y. Tanaka, Z. Ren, T. Sato, K. Nakayama, S. Souma, T. Takahashi, K. Segawa and Y. Ando, Nat. Phys. **8**, 800-803 (2012).
[43] L. Fu, Phys. Rev. Lett. **106**, 106802 (2011).
[44] J. Liu, W. Duan, and L. Fu, Phys. Rev. B **88**, 241303(R) (2013).
[45] L. Fu and C. L. Kane, Phys. Rev. B **76**, 045302 (2007).
[46] See Supplemental Materials for experimental and theoretical method, more data and related analysis, which also includes Refs. [47-51].
[47] P. Zhang, P. Richard, T. Qian, Y.-M. Xu, X. Dai, and H. Ding, Rev. Sci. Ins. **82**, 043712 (2011).
[48] G. Kresse, and J. Furthmüller, Phys. Rev. B. **54**, 11169 (1996).
[49] G. Kresse and J. Hafner, Phys. Rev. B **48**, 13115 (1993).
[50] G. Kresse and D. Joubert, Phys. Rev. B **59**, 1758 (1999).
[51] J. P. Perdew, K. Burke, and M. Ernzerhof, Phys. Rev. Lett. **77**, 3865 (1996).
[52] C. Wang and T. Hughbanks, Inorg. Chem. **34**, 5524 (1995).

∗ Correspondence and requests for materials should be addressed to M.N. (Email: Madhab.Neupane@ucf.edu).